



BNL-NUREG-76748-2006-CP

Finite Element Models for Computing Seismic Induced Soil Pressures on Deeply Embedded Nuclear Power Plant Structures

J. Xu¹, C. Costantino¹, C. Hofmayer¹, H. Graves²

¹Brookhaven National Laboratory, Upton, New York 11973-5000, USA

²US Nuclear Regulatory Commission, Washington, D.C. 20555-0001, USA

Presented at the 2006 ASME Pressure Vessels and Piping Division Conference
Vancouver, BC, Canada
July 23– 27, 2006

Energy Sciences and Technology Department

Brookhaven National Laboratory

P.O. Box 5000

Upton, NY 11973-5000

www.bnl.gov

Notice: This manuscript has been authored by employees of Brookhaven Science Associates, LLC under Contract No. DE-AC02-98CH10886 with the U.S. Department of Energy. The publisher by accepting the manuscript for publication acknowledges that the United States Government retains a non-exclusive, paid-up, irrevocable, world-wide license to publish or reproduce the published form of this manuscript, or allow others to do so, for United States Government purposes.

This preprint is intended for publication in a journal or proceedings. Since changes may be made before publication, it may not be cited or reproduced without the author's permission.

DISCLAIMER

This report was prepared as an account of work sponsored by an agency of the United States Government. Neither the United States Government nor any agency thereof, nor any of their employees, nor any of their contractors, subcontractors, or their employees, makes any warranty, express or implied, or assumes any legal liability or responsibility for the accuracy, completeness, or any third party's use or the results of such use of any information, apparatus, product, or process disclosed, or represents that its use would not infringe privately owned rights. Reference herein to any specific commercial product, process, or service by trade name, trademark, manufacturer, or otherwise, does not necessarily constitute or imply its endorsement, recommendation, or favoring by the United States Government or any agency thereof or its contractors or subcontractors. The views and opinions of authors expressed herein do not necessarily state or reflect those of the United States Government or any agency thereof.

FINITE ELEMENT MODELS FOR COMPUTING SEISMIC INDUCED SOIL PRESSURES ON DEEPLY EMBEDDED NPP STRUCTURES

Jim Xu

Brookhaven National Laboratory
Upton, New York 11973-5000, USA
Tel: 631-344-2183
Email: xu@bnl.gov

Carl Costantino

Brookhaven National Laboratory
Upton, New York 11973-5000, USA
Tel: 631-344-2949
Email: carl@cjccassoc.com

Charles Hofmayer

Brookhaven National Laboratory
Upton, New York 11973-5000, USA
Tel: 631-344-2317
Email: hofmayer@bnl.gov

Herman Graves

US Nuclear Regulatory Commission
Washington, D.C. 20555-0001, USA
Tel: 301-415-5880
Email: hlg1@nrc.gov

ABSTRACT

This paper discusses computations of seismic induced soil pressures using finite element (FE) models for deeply embedded and/or buried (DEB) stiff structures, such as those appearing in the conceptual designs of structures for advanced reactors. For DEB structures, the soil-structure interaction (SSI) effect is expected to have a strong influence on the estimate of the seismic induced soil pressures, especially for stiff structures embedded in soft soil strata. In this paper, two FE models are developed using the SASSI and LS-DYNA computer programs, representing respectively the substructure subtracting method and explicit FE algorithm. SASSI utilizes the wave propagation theory and the principle of superposition to treat the SSI phenomenon. In the LS-DYNA analysis, an attempt is made to apply the direct approach to the SSI effect, which treats the near field soil with an explicit FE mesh that is connected to a transmitting boundary to approximate wave propagation in the half-space.

The structural model used for the study is derived from the characteristics of a conceptual design for an advanced reactor. The structure is founded in a soft soil overburden underlain by a rock and the input seismic motion is specified at rock outcrop and has a zero period acceleration (ZPA) equal to 0.3 g, typical of review level earthquakes for nuclear power plant structures in the Central and Eastern United States. Various depths of burial (DOB) for the structure are considered in the analysis to afford an assessment of the DOB effect on the seismic induced soil pressure estimates determined by these methods. Comparisons and discussions of the analysis results computed by the two approaches are provided.

INTRODUCTION

Although extensive research has been performed to study the phenomenon of soil-structure interaction (SSI), most of the effort has been on improving estimates of the seismic induced in-structure response spectra (ISRS), and less light has been shed on the adequacy of the analytical methods for computing the seismic induced soil pressures on foundations. One reason is that for the current generation of Light Water Reactors (LWR), the structures are primarily founded at or near the ground surface with shallow embedment; therefore, the aspect of adequately computing the seismic induced pressures is not as important as ISRS. A second reason may be due to the fact that the computed ISRS can be validated from available earthquake recordings, as well as from several well organized large scale international test programs (Roesset 1989; Xu, et. al. 2005); the same can not be said with respect to the seismic induced soil pressure data.

Influenced by many benefits such as easy access for refueling, reduction of seismic effects, missile protection and improving site visual activities, several advanced reactor designs have proposed to bury or partially bury reactor structures as one of the major features of their designs (NRC RES, 2002, General Atomics, 1996). Locating safety related structures, systems and components (SSC) below grade could be an effective option to address these issues. Hence, from the regulatory point of view, potential seismic issues pertaining to deeply embedded and/or buried (DEB) structures should be addressed. Issues relating to kinematic interaction and seismic induced earth pressure effects may be more important for DEB structures during seismic events than for structures founded at or near the ground surface. Therefore, on one hand, effort should be made to develop databases for the seismic induced pressures by improving instrumentation technologies for recording earthquake pressure data. On the other hand,

analytical methods and computer programs established primarily for the SSI assessment of the current generation of reactors need to be assessed in the light of the DEB structures. The latter is addressed in this paper.

The study described in this paper is part of a research program sponsored by the U.S. Nuclear Regulatory Commission. Specifically, this study selects two computer programs for the seismic induced pressure calculations, which represent vastly different approaches to SSI phenomenon. The two programs are SASSI (Lysmer, et. al., 1999) and LS-DYNA (LSTC 2001). SASSI represents the substructuring approach to SSI and has been widely accepted in the nuclear industry for SSI analysis. LS-DYNA, which was originally developed for impact problems but expanded in other areas over years, has become a general purpose finite element (FE) program. It does not appear that LS-DYNA has much been used in the area of SSI analysis, but an attempt is made in this study to develop a direct solution for SSI using LS-DYNA. The reason for selecting LS-DYNA is its versatility for interface modeling, which is important for the SSI analysis involving DEB structures.

This paper describes the FE models developed using the SASSI and LS-DYNA computer codes for computing seismic induced soil pressures on DEB structures. The paper is organized in four sections. Section 1 is the introduction and Section 2 provides a description of the DEB structure used in the study, as well as the soil profile and an outcrop input motion. The finite element models and associated assumptions are described in Section 3. Section 4 provides the pertinent comparisons and discussions of seismic induced soil pressures computed with the two programs. Finally, conclusions are provided in Section 5.

DESCRIPTION OF STRUCTURE USED TO EVALUATE SOIL PRESSURE COMPUTATIONS

The structure used to evaluate soil pressure computations is representative of the next generation of NPP structures. The structural model used in this study, as shown in Figure 1, is a reinforced concrete cylinder, which is 46 m long and has an outer diameter of 27 m. The actual structure consists of a variable thickness outer shell and several major walls spanning across the structure providing both flexural rigidity and dividing the space into major areas. This is modeled with a uniform thickness cylindrical shell. The wall thickness (2 m) is selected to match the combined moment of inertia of the actual outer shell and major interior dividing walls.

A major parameter varied in the study is the depth of burial of this model. The model is buried to depths (E) equal to 25% (11.5 m), 50% (23 m), 75% (34.5 m), and 100 % (46 m) of the structural height. These depths of burial (DOB) correspond to DOB / radius ratios (E/R) of 0.85, 1.7, 2.55, and 3.4, respectively. Current technology has been limited to DOB at the lowest end of this scale so that the primary objective of

the study is to determine whether the application of this technology leads to uncertainties when the DOB increases beyond 25 % of the facility height or 85 % of the facility radius.

The stiffness characteristics of the internal equipment are not included in the model. However, the mass of the equipment is lumped with the mass of the cylindrical shell; the combined weight is 92,202 kN. The weights of the basemat and roof are 40,474 kN and 4,450 kN, respectively. The weights have been reduced to some extent from the actual weights to obtain structural frequencies that are likely to be interactive with the SSI frequencies.

The soil profile used in the study is selected to have a shear wave velocity equal to 250 m/s at the surface and 1,000 m/s at a depth of 80 m. Based on a relation between the low strain soil shear modulus and the confined soil pressure (Seed, et al., 1984), the variation of shear wave velocity between the surface and 80 m depth is determined from:

$$V = 250 + 250.78 z^{1/4} \quad (1)$$

The soil column is founded on bedrock at a depth of 80 m having a shear wave velocity equal to 2,000 m/s, a density equal to 17.28 kN/m³, and a material damping equal to 2 % of critical.

The input motion is specified at a rock outcrop and standard convolution procedures for vertically propagating horizontal shear waves are used to compute the free field motions within the soil column. For this generic study, the characteristic event was defined as a magnitude 7 earthquake located at a distance of 25 kilometers from the site. The peak acceleration associated with this dominant event was selected as 0.3 g. Spectra of the rock outcrop motion and the motion at various depths in the soil column are shown on Fig. 2.

DESCRIPTION OF FINITE ELEMENT MODELS

The detailed SASSI FE model uses the sub-structuring method as implemented in SASSI2000 developed by Lysmer and his team at U.C. Berkeley (Lysmer, 1999). The SASSI program has gone through extensive improvement over years. In addition to the sub-structuring methods such as the flexible volume, flexible boundary and rigid boundary methods as in the previous versions, SASSI 2000 implemented a new subtraction method, which is used to carry out the SSI response calculations. Of course, SASSI is a linear code so that non linear effects such as separation of the soil from the wall or sliding of the soil along the wall cannot be included. Although non-linear effects may be approximately estimated (Xu, et. al., 2005), perfect bonding is assumed at the soil-wall interface for making comparisons on a consistent basis with the LS-DYNA results.

In the detailed SASSI FE models, the portion of the structure below the ground surface is modeled with explicit finite elements (e.g., 3-D bricks and shells), while the superstructure above the ground surface is represented with simple lumped masses and 3-D beams. The models are developed for the four different embedment conditions, ranging from shallow embedment to full burial. A typical SASSI DEB model is shown in Fig. 3. As shown in this figure, the basemat is modeled with brick elements and the sidewalls and internals are modeled with shell elements. The base of the superstructure is connected to the sidewalls by rigid links to simulate the rigid diaphragm of the floor expected to exist at grade level. Two layers of solid soil elements are placed radially outside the structure so that soil pressures may be evaluated.

The LS-DYNA program is used to develop the finite element models for the unbounded SSI system. The models consider various depths of embedment. The difficulties encountered in modeling the wave propagation in an unbounded soil with a deeply embedded structure are: 1) finite element modeling of the half-space medium and 2) assumptions made to associate the structural wall and the surrounding soil at the interfaces.

In order to represent the half-space soil medium with explicit finite elements, the near field in which the SSI effect is expected is modeled with explicit 3-D brick type elements. The lateral boundary of the near field model should be extended sufficiently far such that the outgoing wave due to the structural vibration diminishes drastically at the boundary. To prevent any reflection of outgoing waves at the boundary, a series of artificial viscous dampers are attached to the boundary. In LS-DYNA, the approach developed by Lysmer and Kuhlemeyer [Lysmer, 1969] was implemented, in which viscous normal and shear stresses are applied to the boundaries in a manner as defined in the following equations:

$$\sigma_{\text{normal}} = -\rho c_d V_{\text{normal}}$$

$$\sigma_{\text{shear}} = -\rho c_s V_{\text{tangential}}$$

where ρ , c_d , and c_s are the material density, material longitudinal and shear wave velocities of the transmitting media. These equations reveal that the magnitude of these stresses at the boundaries is proportional to the particle velocities in the normal (V_{normal}) and in the tangential ($V_{\text{tangential}}$) directions. The Lysmer's dampers placed on the artificial boundary are effective in reducing unwanted wave reflections if the boundary of the finite element mesh is sufficiently far outward. However, in doing so, the size of the near field finite element mesh is increased significantly and so is the cost of running the dynamic analysis. The exact stress field on the soil boundary of the given problem is a function of frequency dependent dampers and springs. However, as shown by Wolf [Wolf, 1999], the springs dominate the boundary

stress field in low frequencies and near field, and as the frequency and the mesh boundary approaches infinity, the boundary stress field becomes a function of dampers only. Therefore, for a finite mesh of the unbounded soil medium, an improved transmitting boundary can be developed by applying a combination of springs and dampers to the boundary. Wolf [Wolf, 1999] and Luco [Luco, 2004] have proposed such advanced transmitting boundaries. Figure 4 presents the finite element SSI model for the 50% embedment case and Figure 5 shows a zoom-in view of the structure and the surrounding soils. Note that the circular boundary placed on the lateral end of the SSI system mesh is to ensure proper wave propagation near the boundary and to avoid the so called "corner effect" which would occur if a rectangular boundary is imposed on the mesh.

To be consistent with the SASSI models regarding the soil/structure interface, the tied interface condition is imposed in the LS-DYNA models in that the soil/structure interface is tied together using the LS-DYNA keyword "Contact_tied_surface_to_surface".

An in-column seismic motion converted from the outcrop input in the form of an acceleration time history is imposed on the SSI system mesh at the depth of 80m. The base of the mesh, which is at the depth of 84m, is attached to the Lysmer dampers as described above.

The LS-DYNA SSI model consists of at least a quarter million nodes and a quarter million elements. The seismic analysis is performed using the explicit time integration algorithm with the Rayleigh damping specified with each soil layer and within the structure. Seismic analysis for the explicit finite element models with the contact interface features is very time consuming. However, the use of parallel processing with multiple cpu's can substantially reduce the calculation time.

COMPARISONS OF ANALYSIS RESULTS BETWEEN SASSI AND LS-DYNA MODELS

To illustrate the modeling effect using different SSI analysis approaches on seismic induced pressures, the vertical distributions of the instant soil pressures on the structural wall are plotted and compared. The instant of time is selected which corresponds to time when the mid-height soil wall pressure reaches the peak value. To examine the overall performance in the frequency content of the soil pressures, the Fourier spectra of the normal soil pressure in the head-on soil element near the mid-height of the structural wall for different depths of burial (DOB) are computed and compared between SASSI and LS-DYNA. The following provides an assessment of the modeling effect on the seismic induced soil pressures.

Figure 6 presents the vertical distribution of the soil wall pressures computed with the SASSI and LS-DYNA models for 25% DOB. As shown in the picture, the wall depth is

represented by the vertical axis expressed as a percentage of the DOB of the structure and the soil stresses on the wall are expressed in the horizontal axis in the unit of kN/m^2 . The symbols S_{rr} and S_{rz} represent the normal soil pressure and vertical shear computed in the head-on soil elements, while the symbol S_{rt} is the meridian shear computed in the soil elements 90 degree counterclockwise from the head-on location.

For the 25% DOB, it is readily observed from Figure 6 that very good matches are obtained for all three soil stress components. Especially for the normal soil pressures, SASSI and LS-DYNA computed nearly identical vertical distribution both in shape and magnitude. The fact that these soil stress comparisons show remarkable agreement is important, because of the vastly different analytical approaches implemented in the SASSI and LS-DYNA programs.

The comparisons of the vertical soil pressure distributions for the 50% DOB are provided in Figure 7. In this figure, the SASSI and LS-DYNA computed soil pressure vertical distributions are fairly close to each other and the overall comparison between SASSI and LS-DYNA is comparable to the 25% DOB case.

For the 75% DOB, the comparisons of vertical soil pressure distributions between SASSI and LS-DYNA are presented in Figure 8. As depicted in this figure, more oscillatory behavior is observed of the vertical soil pressure distributions than the shallower cases presented above. Furthermore, the normal pressure and vertical shear are still closely traced between the SASSI and LS-DYNA results, while meridian shear distributions exhibit vastly different behavior between the SASSI and LS-DYNA calculations.

Finally, Figure 9 depicts the comparisons of the vertical soil pressure distributions between SASSI and LS-DYNA for the 100% DOB. The comparisons of the vertical distributions of the soil pressures are also comparable to the 25% and 50% DOB cases.

To further investigate the soil pressure responses calculated using SASSI and LS-DYNA, the soil pressures time history in the head-on soil element near the mid-height embedded wall are transformed into the frequency domain, and the Fourier spectra of the soil pressure are plotted and compared between the LS-DYNA models and the SASSI models. Before making the comparison, both the SASSI and LS-DYNA Fourier spectra for soil pressure time history are calculated and then smoothed with a 0.5Hz triangular window function.

Figures 10 through 13 show the comparisons of the smoothed Fourier spectra of the computed soil pressure between the SASSI and the LS-DYNA models for the 25%, 50%, 75% and 100% DOB cases. These figures indicate close

matches of the frequency content between the two model results, except for the 100% DOB case where much higher amplitude is shown for the LS-DYNA estimate than the SASSI result between 3-8 Hz. Furthermore, the Fourier spectrum comparisons have clearly demonstrated the similar frequency characteristics of the pressure responses calculated from the two models.

CONCLUSIONS

A study was performed to provide an assessment of the sensitivity to the seismic induced soil pressure calculations when vastly different SSI methods are employed. SASSI and LS-DYNA, which represent two vastly different SSI approaches, are used for the study. The analysis results in terms of the vertical soil wall pressures are calculated and compared between the SASSI and LS-DYNA results. Fourier spectra of the normal soil wall pressures are also computed and compared between SASSI and LS-DYNA. The analytical results consider four depths of foundation embedment, ranging from shallow (25%) to fully buried (100%).

Based on the results and discussions as described in this paper, the conclusions can be drawn that in general, the SSI methods for calculating the seismic soil wall pressures are stable and yield comparable pressure responses. Further, when the linear assumption is made, the SSI methodologies can practically be applied from shallow to fully buried structural configurations. However, this study was unable to validate the linear SSI methods when applied to strong ground motion response analyses. In these cases, non-linear phenomena such as soil/wall separations, and localized soil material nonlinearity may influence the computed SSI response, and the corresponding analytical methods may require further assessment through correlations with field or laboratory strong ground motion data.

DISCLAIMER NOTICE

This work was performed under the auspices of the U.S. Nuclear Regulatory Commission, Washington, D.C. The findings and opinions expressed in this paper are those of the authors, and do not necessarily reflect the views of the U.S. Nuclear Regulatory Commission or Brookhaven National Laboratory.

REFERENCES

- General Atomics, 1996, "GT-MHR, Conceptual Design Description report."
- LSTC, "LS-DYNA User's Manual," vols. 1 & 2, Version 960, March 2001.
- Luco, J. E., "Approximate External Boundaries for Truncated Models of Unbounded Media," Proceedings, 3rd UJNR Workshop of Soil-Structure Interaction, Menlo Park, CA, March 2004

Lysmer, J., et al., 1999, "SASSI2000 – Theoretical Manual," Revision 1, Geotechnical Engineering, University of California, Berkeley.

Lysmer, J., et al., "Finite Dynamic Model for Infinite Media," J. Eng. Mech. Div. ASCE, 589-877, 1969.

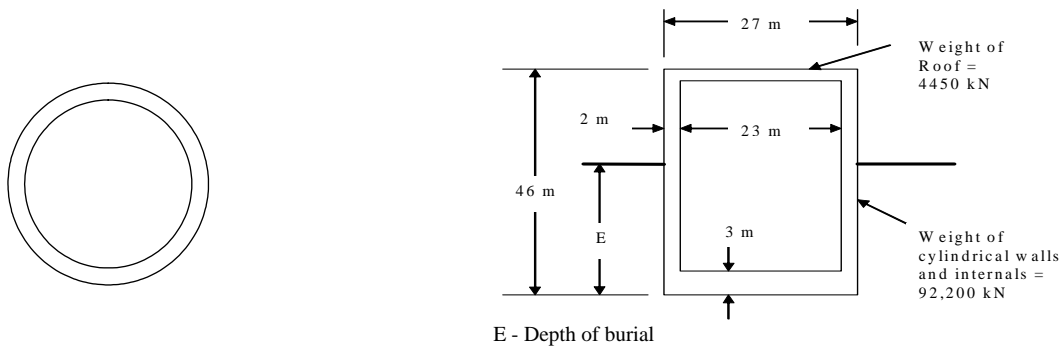
NRC RES Advanced Reactor Research Plan, Rev. 1 Draft report, ML021760135, June 2002.

Roesset, J. M., "Perspectives on Soil Structure Interaction Analysis," Proceedings of EPRI/NRC/TPC Workshop on Seismic Soil-Structure Analysis, Lotung, Taiwan," Vol. 1, EPRI NP-6154, March 1989.

Seed, H.B., et al., 1984, "Soil Moduli and Damping Factors for Dynamic Response Analysis of Cohesionless Soils," Report No. UCB/EERC-8914, Earthq. Eng. Research Center, University of California, Berkeley, CA.

Wolf, J. P., et al., Finite-Element Modeling of Unbounded Media, John Wiley & Sons, England, June 1999.

Xu, J., et al., "Assessment of Seismic Analysis Methodologies for Deeply Embedded Nuclear Power Plant Structures," NUREG/CR Report, 2005.



(a) Cross Section

(b) Elevation

Figure 1. Structure Considered in the Study

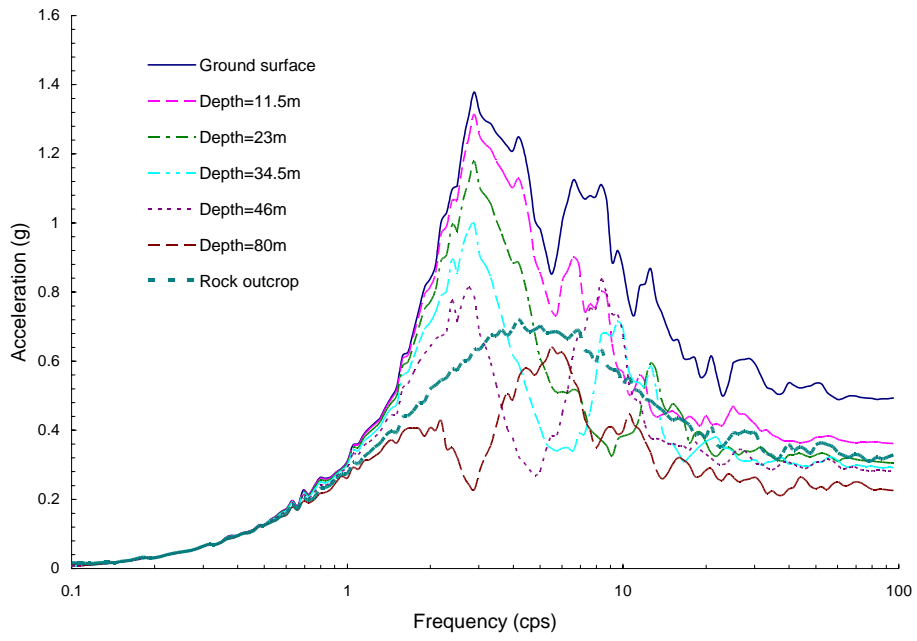


Figure 2. Site Free-Field Response Spectra

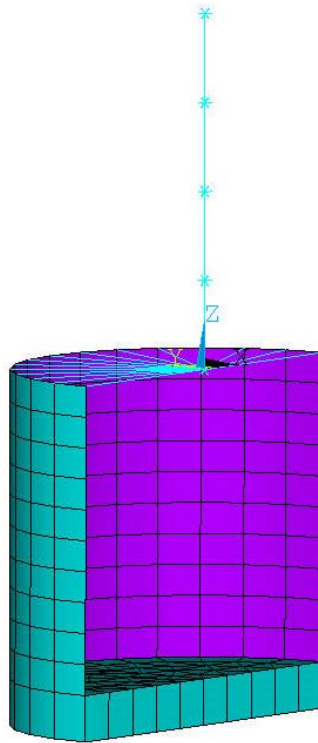


Figure 3. SASSI Structural Model

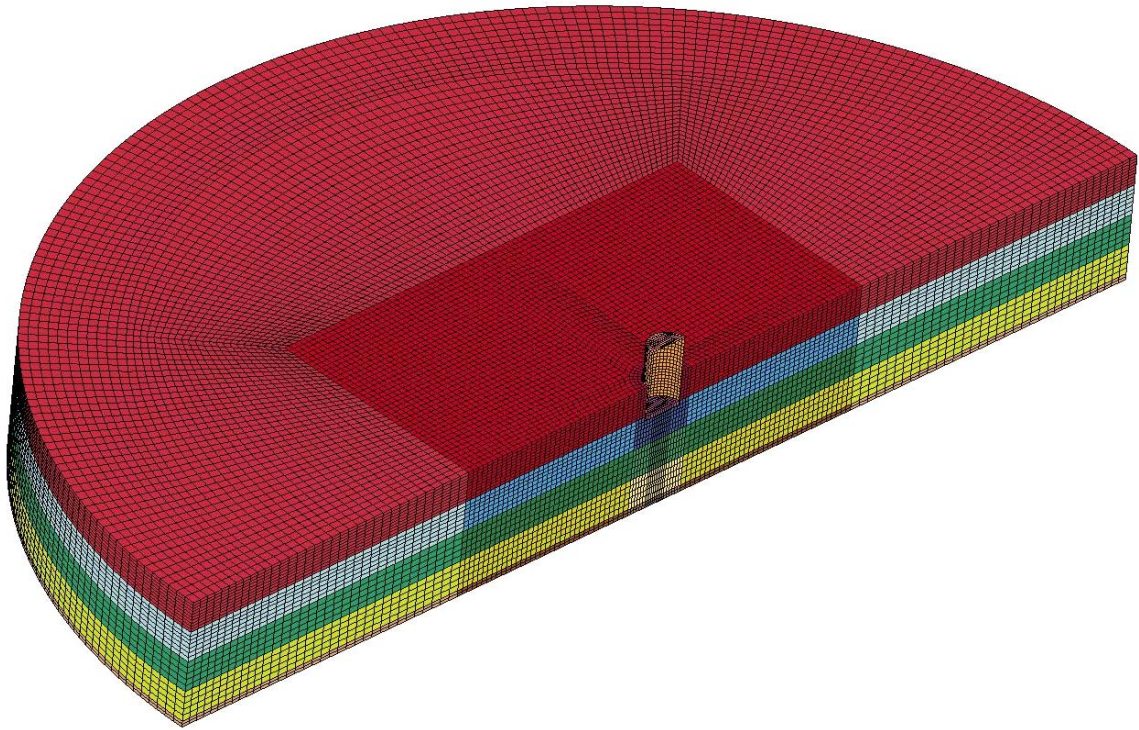


Figure 4. The LS-DYNA Model for 50% Embedment

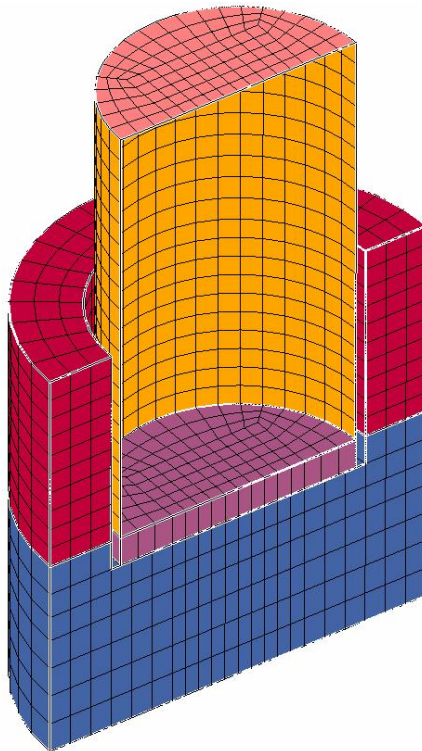


Figure 5. Zoom-in View of the Structure and Surrounding Soil in LS-DYNA Model for the 50% Embedment

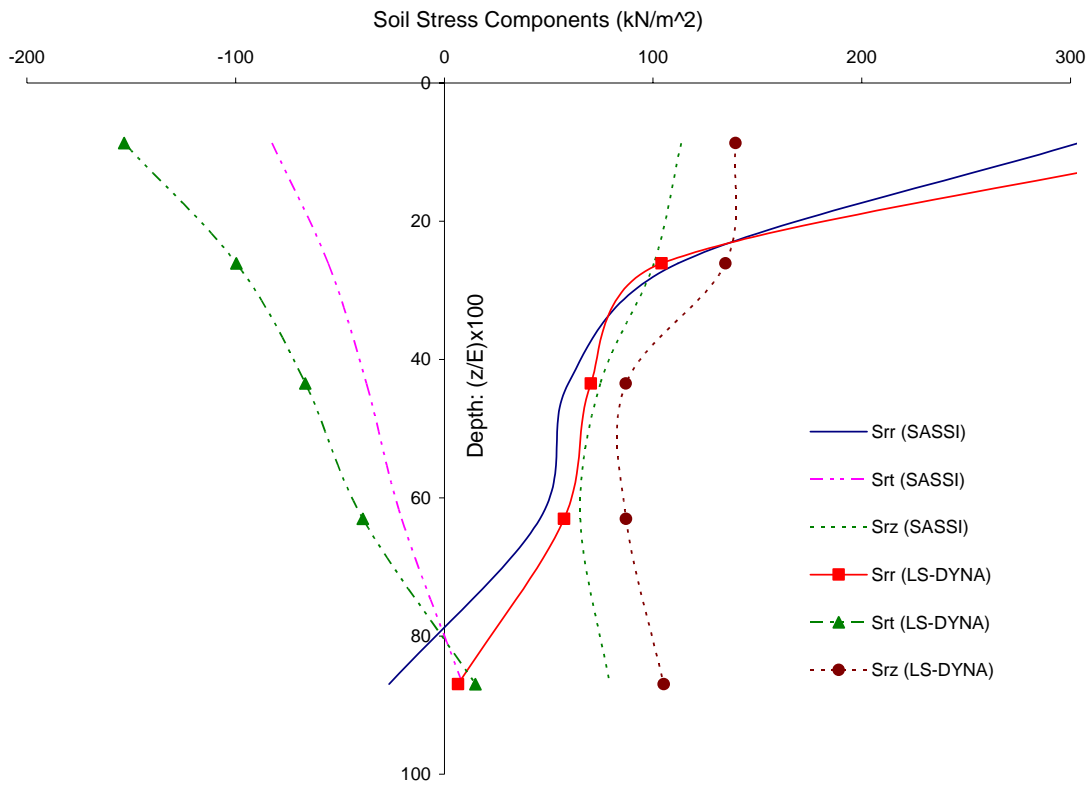


Figure 6. Comparisons of Vertical Distributions of Soil Pressure for 25% DOB

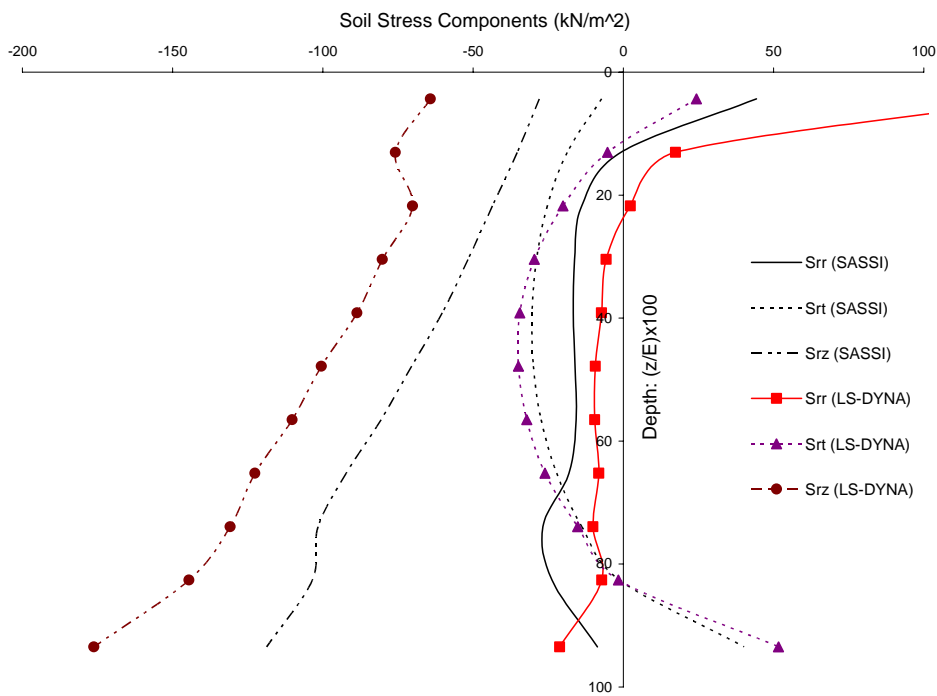


Figure 7. Comparisons of Vertical Distributions of Soil Pressure for 50% DOB

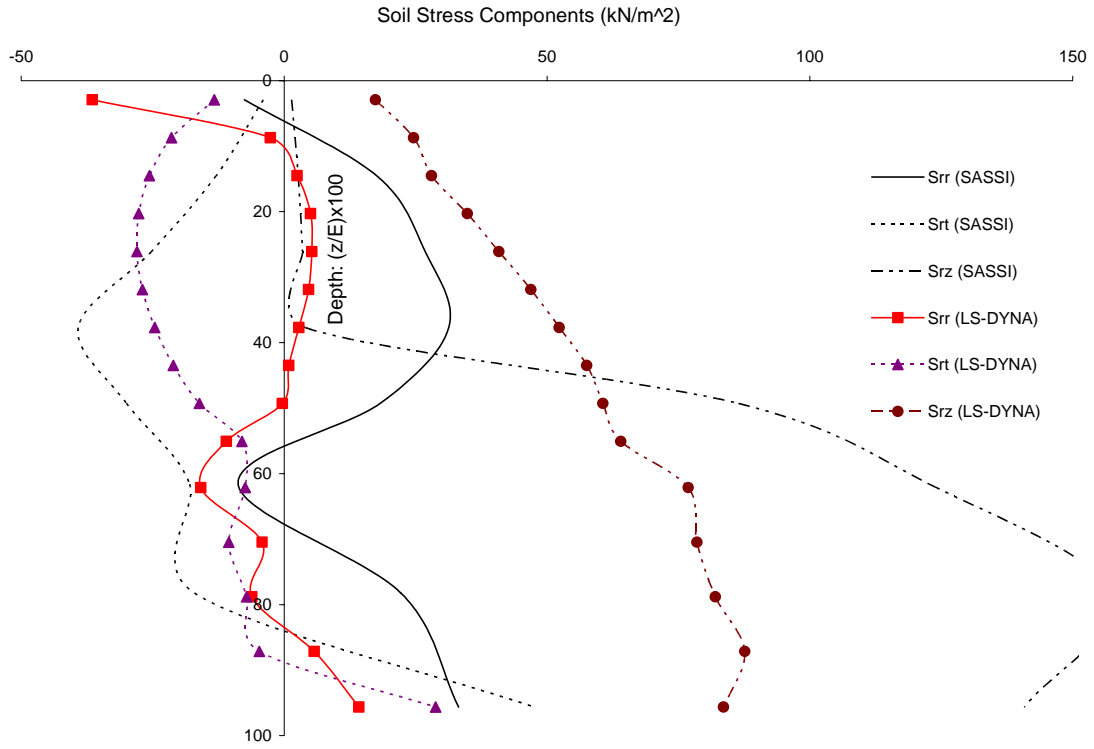


Figure 8. Comparisons of Vertical Distributions of Soil Pressure for 75% DOB

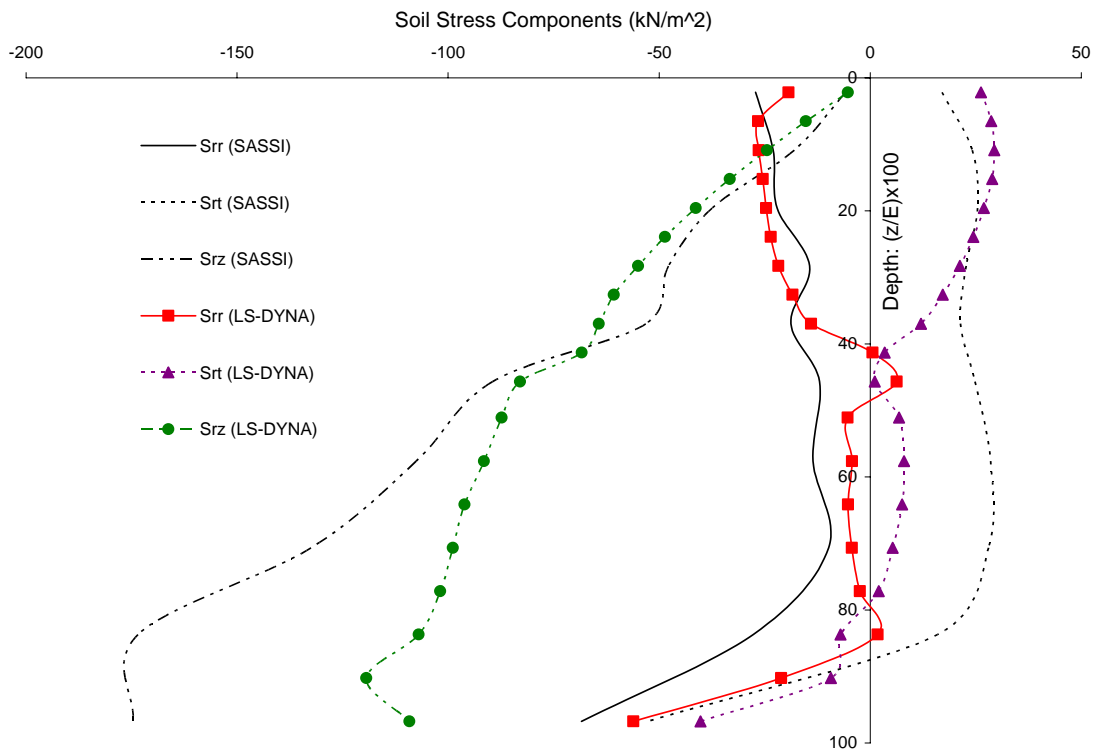


Figure 9. Comparisons of Vertical Distributions of Soil Pressure for 100% DOB

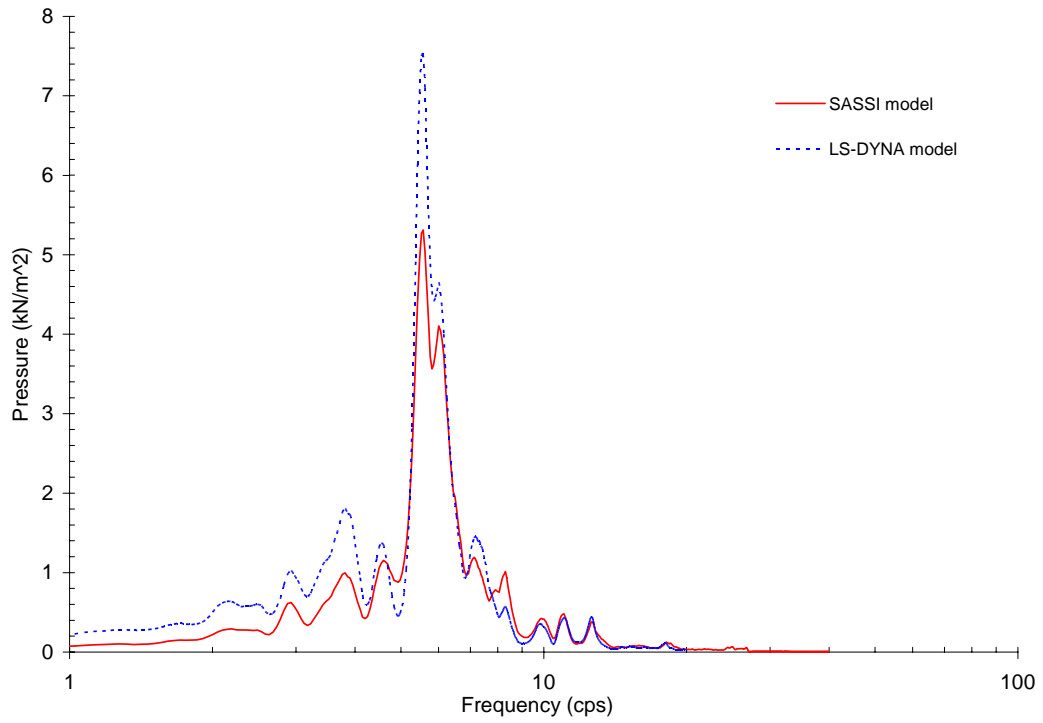


Figure 10. Fourier Spectra of Soil Pressure Computed at the Head-on Soil Element near Mid-Height Embedded Wall for 25% DOB

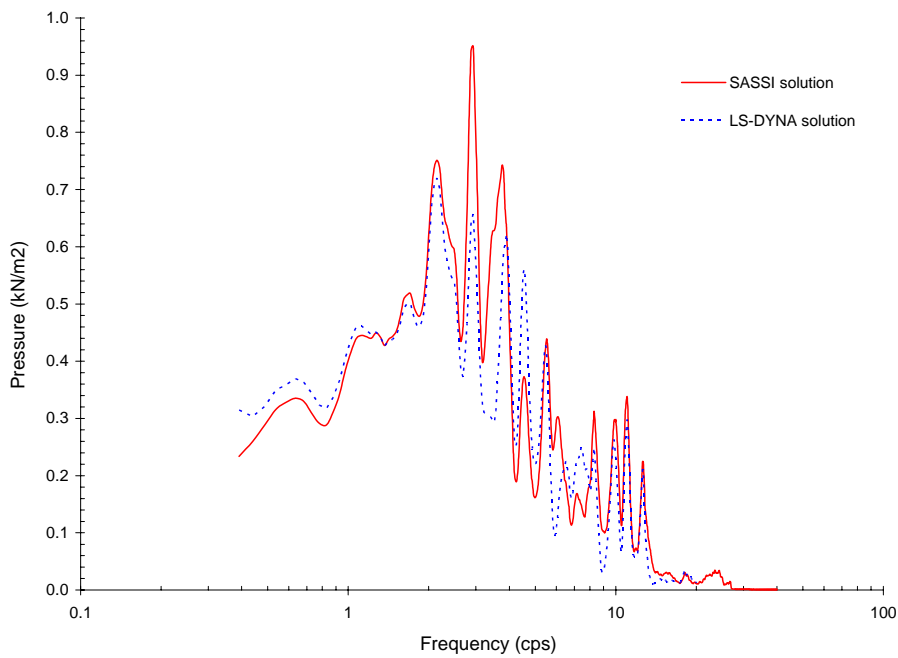


Figure 11. Fourier Spectra of Soil Pressure Computed at the Head-on Soil Element near Mid-Height Embedded Wall for 50% DOB

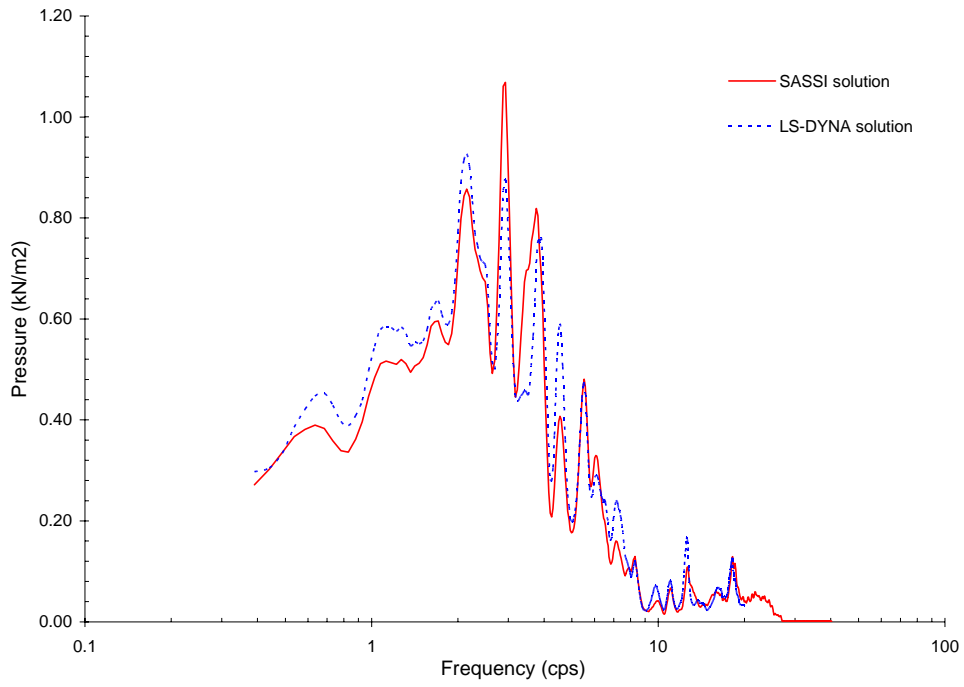


Figure 12. Fourier Spectra of Soil Pressure Computed at the Head-on Soil Element near Mid-Height Embedded Wall for 75% DOB

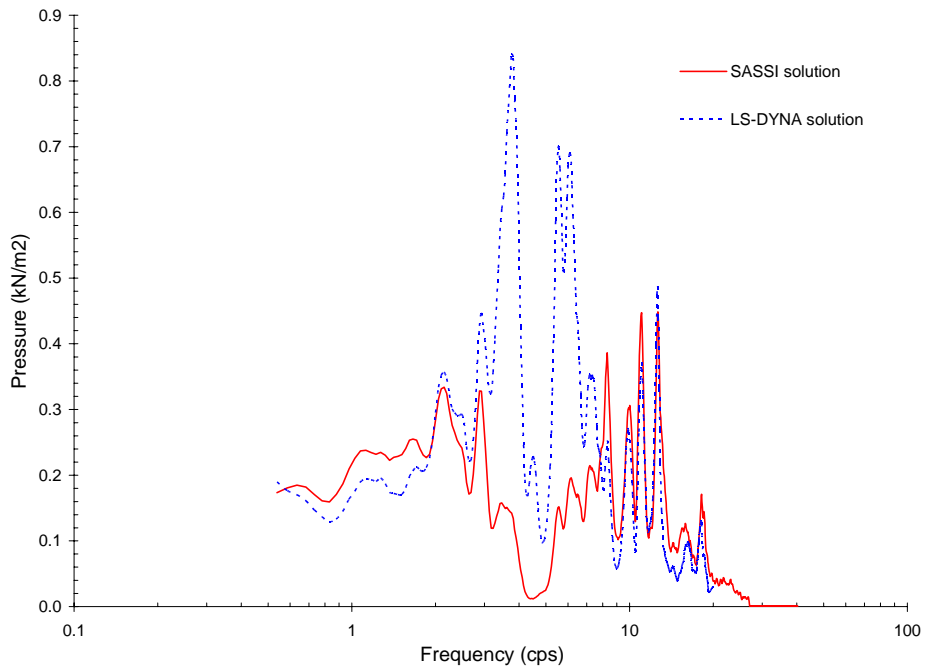


Figure 13. Fourier Spectra of Soil Pressure Computed at the Head-on Soil Element near Mid-Height Embedded Wall for 100% DOB